



RESEARCH MEMORANDUM

FREE-FLIGHT INVESTIGATION AT TRANSONIC AND SUPERSONIC
SPEEDS OF THE ROLLING EFFECTIVENESS OF A PARTIAL-SPAN
AILERON ON AN INVERSELY TAPERED SWEPTBACK WING

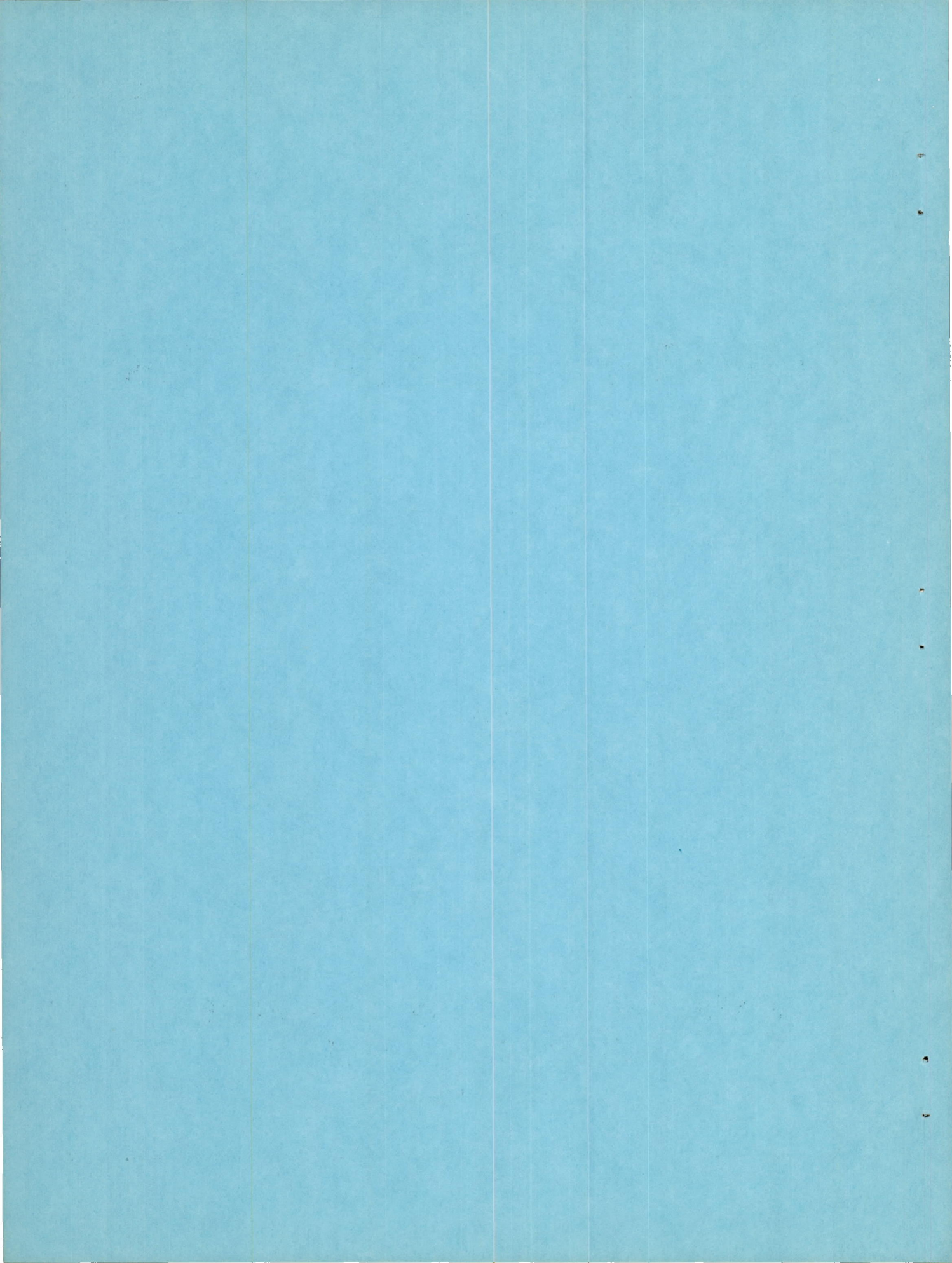
By H. Kurt Strass, E. M. Fields, and E. D. Schult

Langley Aeronautical Laboratory
Langley Air Force Base, Va.

NATIONAL ADVISORY COMMITTEE
FOR AERONAUTICS

WASHINGTON

May 1, 1950



NATIONAL ADVISORY COMMITTEE FOR AERONAUTICS

RESEARCH MEMORANDUM

FREE-FLIGHT INVESTIGATION AT TRANSONIC AND SUPERSONIC
SPEEDS OF THE ROLLING EFFECTIVENESS OF A PARTIAL-SPAN
AILERON ON AN INVERSELY TAPERED SWEEPBACK WING

By H. Kurt Strass, E. M. Fields, and E. D. Schult

SUMMARY

An investigation of the rolling effectiveness at transonic and supersonic speeds of an inversely tapered sweptback wing having a 10-percent-thick cambered airfoil section and outboard partial-span controls has been made by means of rocket-propelled test vehicles. The variation of rolling effectiveness with Mach number was smooth with the exception of a small discontinuity which occurred at a Mach number of 0.95 for the models with the controls deflected 5° or -5° . The control effectiveness decreased by approximately 60 percent over the range from Mach number 0.8 to 1.6. Positive and negative aileron deflections were equally effective in producing roll throughout the entire speed range. The angle of attack for zero lift of the cambered airfoil was indicated to decrease smoothly from a negative value of approximately 1° at subsonic speeds to approximately 0° at a Mach number of 1.6.

INTRODUCTION

A wing-aileron configuration having inverse taper ($\lambda = 1.63$), aspect ratio of 3.1, 40° sweepback of the 50-percent free-stream chord line, and employing a 10-percent-thick low-drag-type airfoil normal to the 50-percent free-stream chord line was tested as a part of the wing-aileron rolling-effectiveness program now being conducted by the Langley Pilotless Aircraft Research Division utilizing rocket-propelled test vehicles in free flight. The true-contour flap-type ailerons were hinged at the 73.04-percent free-stream chord line and extended over 38.7 percent of the semispan and simulated sealed controls in that there was no gap at the hinge line. The investigation was made by means of the free-flight technique described in references 1 and 2 and data were obtained over the Mach number range from approximately 0.7 to 1.70 at

Reynolds numbers from 2.5×10^6 to 8.5×10^6 . Six models were tested; two with 5° aileron deflection, two with 0° aileron deflection, and two with -5° aileron deflection.

SYMBOLS

A	aspect ratio (b^2/S_1)
b	diameter of circle swept by wing tips, when body is rotated about its longitudinal axis, feet
c	chord of wing parallel to free stream, feet
C_{DT}	total-drag coefficient, based on total exposed wing area S
M	free-stream Mach number
m	concentrated couple, applied near wing tip in plane normal to wing-chord plane, inch-pounds
p	model rate of roll, radians per second
$pb/2V$	wing-tip helix angle, radians
$\Delta\left(\frac{pb}{2V}\right)_{1w}$	$pb/2V$ due to wing incidence, radians
$\Delta\left(\frac{pb}{2V}\right)_{\delta_a}$	$pb/2V$ due to aileron deflection alone, radians
R	Reynolds number
S	total exposed wing area (three wing panels), square feet
S_1	area of two wing panels taken to the center line, square feet
α_0	wing angle of attack for zero lift, measured from chord line, degrees
θ	angle of wing twist produced by m at any section along wing span normal to wing-chord plane, radians

θ/m	wing torsional-stiffness parameter, radians per inch-pound
λ	ratio of chord of wing at tip to chord of wing at model center line obtained by extending leading and trailing edges to model center line
i_w	incidence of wing measured in free-stream direction, average for three wings, degrees
δ_a	deflection of each aileron measured in free-stream direction, average for three wings, degrees

TEST VEHICLES AND TESTS

The geometrical characteristics of the test vehicles are given in table I. The general arrangement of the test vehicles is shown in the photograph presented as figure 1 and the sketch in figure 2. The section airfoil ordinates of A-A and B-B in figure 2 are given in table II.

The wings of the test models were stiffened by means of 0.020-inch steel plates glued into the upper and lower surfaces. In addition, a central core of $\frac{3}{32}$ -inch aluminum alloy was used to provide additional protection to the leading and trailing edges of the wings and to stiffen the ailerons to prevent movement under the air loads encountered in flight. The torsional characteristics of the test wings using this type of construction are presented in figure 3. Based on unpublished data, the test wings were sufficiently rigid to restrict the loss in control effectiveness to approximately 10 percent of the rigid-wing value at a maximum Mach number of 1.70.

Because of the relatively small moment of inertia about the roll axis, the measured values of $pb/2V$ are substantially steady-state values even though the test vehicles experienced an almost continuous rolling acceleration or deceleration. The data presented herein have not been corrected for inertia effects. Except for abrupt changes of $pb/2V$ with Mach number, which usually occur in the region between $M = 0.90$ to 0.97 , this correction is estimated to be within 3 percent.

Due to the fact that the airfoil section used was cambered, it was necessary to obtain data for the wing-aileron configuration with the control set at 0° in order to separate the effect of camber from the effect of the aileron. In addition, data were also obtained at a negative aileron setting in order to determine whether the control

effectiveness was independent of the direction of aileron setting. The wings were set into the body of the test vehicle in such a manner that the lift due to the camber caused the models to rotate in a clockwise direction as seen from the rear. Positive aileron deflection was considered to be in a direction that would tend to increase the rotation due to camber.

CORRECTIONS

Due to limitations in constructional accuracy, resulting in small deviations from design values, the data were corrected to a common aileron setting and zero incidence to allow direct comparison between models. The rolling-effectiveness parameter $pb/2V$ was assumed to vary linearly with aileron deflection. Errors in incidence were corrected by assuming that a steady-state rolling condition existed where the rolling moment caused by incidence was equal to the damping moment. In addition, the lift-curve slope at any position along the span due to incidence was assumed to be equal to the lift-curve slope due to damping and the resulting general equation is as follows:

$$\Delta \left(\frac{pb}{2V} \right)_{i_w} = \frac{2i_w}{57.3} \frac{1 + 2\lambda}{1 + 3\lambda} = 0.0253i_w$$

The correction for incidence was assumed to be constant throughout the entire Mach number range and has been verified experimentally, except for the region $M \approx 0.85$ to $M \approx 1.0$. (See reference 3.) Listed in table III are the measured values of incidence i_w and aileron deflection δ_a . The $pb/2V$ curves presented have been corrected to $i_w = 0^\circ$ and $\delta_a = 5^\circ$ by the method just described.

ACCURACY

Based upon previous experience the accuracy of the test results is estimated to be within the following limits:

$pb/2V$ (due to limitations on model constructional accuracy)	± 0.0025
$pb/2V$ (due to limitations on instrumentation)	± 0.0015
C_{D_T}	± 0.002
M	± 0.01

RESULTS

The Reynolds number range for the tests is shown in figure 4. The results of the present investigation are presented in figures 5 and 6. The total-drag coefficient C_{D_T} and the rolling-effectiveness parameter $pb/2V$ for aileron deflections of 5° , -5° , and 0° are presented in figure 5 as a function of Mach number. There was no measurable change in total-drag coefficient between the models with 0° and -5° aileron deflection although a considerable increase in drag was evident for the positive aileron setting in the supersonic range. The variation of $pb/2V$ with Mach number was smooth with the exception of a small discontinuity at $M = 0.95$ for the models with the controls deflected 5° or -5° .

The effectiveness of the aileron in producing roll is shown in figure 6, which gives the incremental change in rolling effectiveness for the positive and negative aileron deflection from the neutral setting. The data are plotted in the same direction to facilitate comparison. It can be seen that the effectiveness was essentially independent of direction of aileron deflection over the entire Mach number range investigated with a gradual loss in effectiveness of 60 percent being experienced in going from approximately $M = 0.8$ to $M = 1.6$.

As mentioned previously, the rolling velocity obtained with the controls neutral is an indication of the effectiveness of the camber in producing lift, or in the present case, rolling moment. From figure 5, the variation of $pb/2V$ with Mach number for models 1 and 2 shows that the effectiveness of the camber decreased continuously with increasing Mach number until at a Mach number of 1.6, the effectiveness was zero. The loss in effectiveness of camber in producing roll can be expressed as a shift in the angle of zero lift of the wing by applying the incidence correction factor given previously. This application has been made and the results are shown in figure 6. The camber is seen to be equivalent to approximately 1° incidence at subsonic speeds decreasing to approximately 0° at the highest supersonic speeds. The fact that the angle of zero lift changes smoothly throughout the speed range indicates that an abrupt change in the angle of trim due to this reason is unlikely to occur.

CONCLUSIONS

The following conclusions may be drawn from an investigation of the rolling effectiveness at transonic and supersonic speeds of an

inversely tapered sweptback wing having a 10-percent-thick cambered airfoil section and outboard partial-span controls:

1. The variation of rolling effectiveness with Mach number was smooth with the exception of a small discontinuity at a Mach number of 0.95 for the test vehicles with positive and negative aileron deflections of 5° . There was a 60-percent loss in effectiveness between Mach numbers of 0.8 and 1.6.

2. Positive and negative aileron deflections of 5° were equally effective in producing roll throughout the entire speed range.

3. The angle of attack for zero lift of the cambered airfoil was indicated to decrease smoothly from a negative value of approximately 1° at subsonic speeds to approximately 0° at a Mach number of 1.6.

Langley Aeronautical Laboratory
National Advisory Committee for Aeronautics
Langley Air Force Base, Va.

REFERENCES

1. Sandahl, Carl A., and Marino, Alfred A.: Free-Flight Investigation of Control Effectiveness of Full-Span 0.2-Chord Plain Ailerons at High Subsonic, Transonic, and Supersonic Speeds to Determine Some Effects of Section Thickness and Wing Sweepback. NACA RM L7D02, 1947.
2. Sandahl, Carl A.: Free-Flight Investigation of the Rolling Effectiveness of Several Delta Wing-Aileron Configurations at Transonic and Supersonic Speeds. NACA RM L8D16, 1948.
3. Strass, H. Kurt, and Fields, Edison M.: Flight Investigation of the Effect of Thickening the Aileron Trailing Edge on Control Effectiveness for Sweptback Tapered Wings Having Sharp- and Round-Nose Sections. NACA RM L9L19, 1950.

TABLE I
 GEOMETRIC CHARACTERISTICS OF TEST VEHICLES

Wing semispan, ft	0.99
Total exposed wing area (3 wing panels), S, sq ft	1.563
Area of two wing panels taken to model center line, S_1 , sq ft	1.261
Aspect ratio, A	^a 3.1
Taper ratio, λ	^a 1.63
Sweepback of 50-percent free-stream chord, deg	40
Position of inboard end of aileron, percent semispan	55
Position of outboard end of aileron, percent semispan	93.7
Ratio of aileron span to wing span	0.387
Average moment of inertia about roll axis, slug-ft ²	0.083
Airfoil profile normal to 50-percent free-stream chord, (Republic Aviation Corp. designation)	R-4, 40-1710 x
Body length, in.	56
Body diameter, in.	5
Body contour	See reference 1

^aObtained by extending leading and trailing edges to model center line.

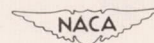


TABLE II

ORDINATES OF AIRFOIL SECTIONS IN FIGURE 2

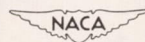
[All distances measured in inches]

Section A-A			Section B-B		
Station	Ordinate		Station	Ordinate	
	Upper surface	Lower surface		Upper surface	Lower surface
0	0	0	0	0	0
.046	.061	.050	.033	.043	.035
.069	.074	.061	.050	.052	.043
.115	.096	.079	.084	.068	.055
.229	.136	.109	.167	.097	.078
.458	.191	.149	.335	.138	.108
.687	.232	.178	.502	.169	.129
.916	.265	.200	.669	.193	.145
1.374	.315	.232	1.003	.230	.169
1.832	.352	.254	1.338	.257	.186
2.290	.379	.269	1.672	.277	.197
2.749	.396	.278	2.007	.289	.203
3.207	.407	.282	2.341	.297	.206
3.665	.411	.282	2.676	.300	.206
4.123	.407	.276	3.010	.298	.202
4.581	.397	.265	3.345	.290	.194
5.039	.380	.249	3.679	.278	.182
5.497	.356	.230	4.014	.260	.168
5.955	.327	.205	4.348	.239	.149
6.413	.292	.177	4.682	.213	.129
6.871	.252	.146	5.017	.184	.107
7.329	.208	.115	5.351	.152	.084
7.788	.161	.082	5.686	.117	.060
8.246	.111	.050	6.020	.081	.036
8.704	.058	.022	6.355	.042	.016
9.162	.007	.007	6.689	.007	.007
L.E. radius: 0.035 T.E. radius: 0.007			L.E. radius: 0.025 T.E. radius: 0.007		



TABLE III
MEASURED VALUES OF i_w AND δ_a

Model	i_w (deg)	δ_a (deg)
1	0.05	0
2	.01	0
3	-.03	-4.74
4	-.03	-4.74
5	.01	5.04
6	.02	5.08



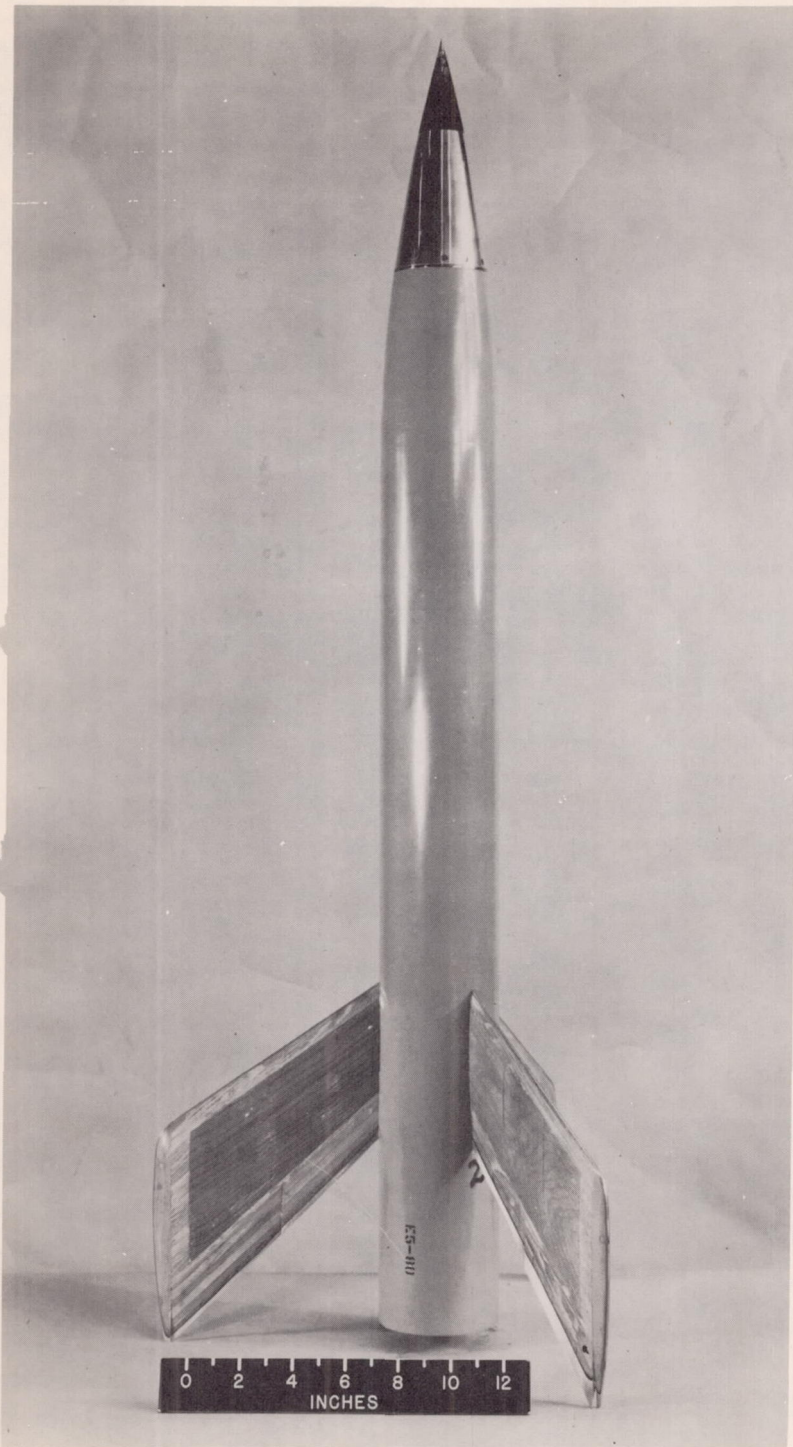
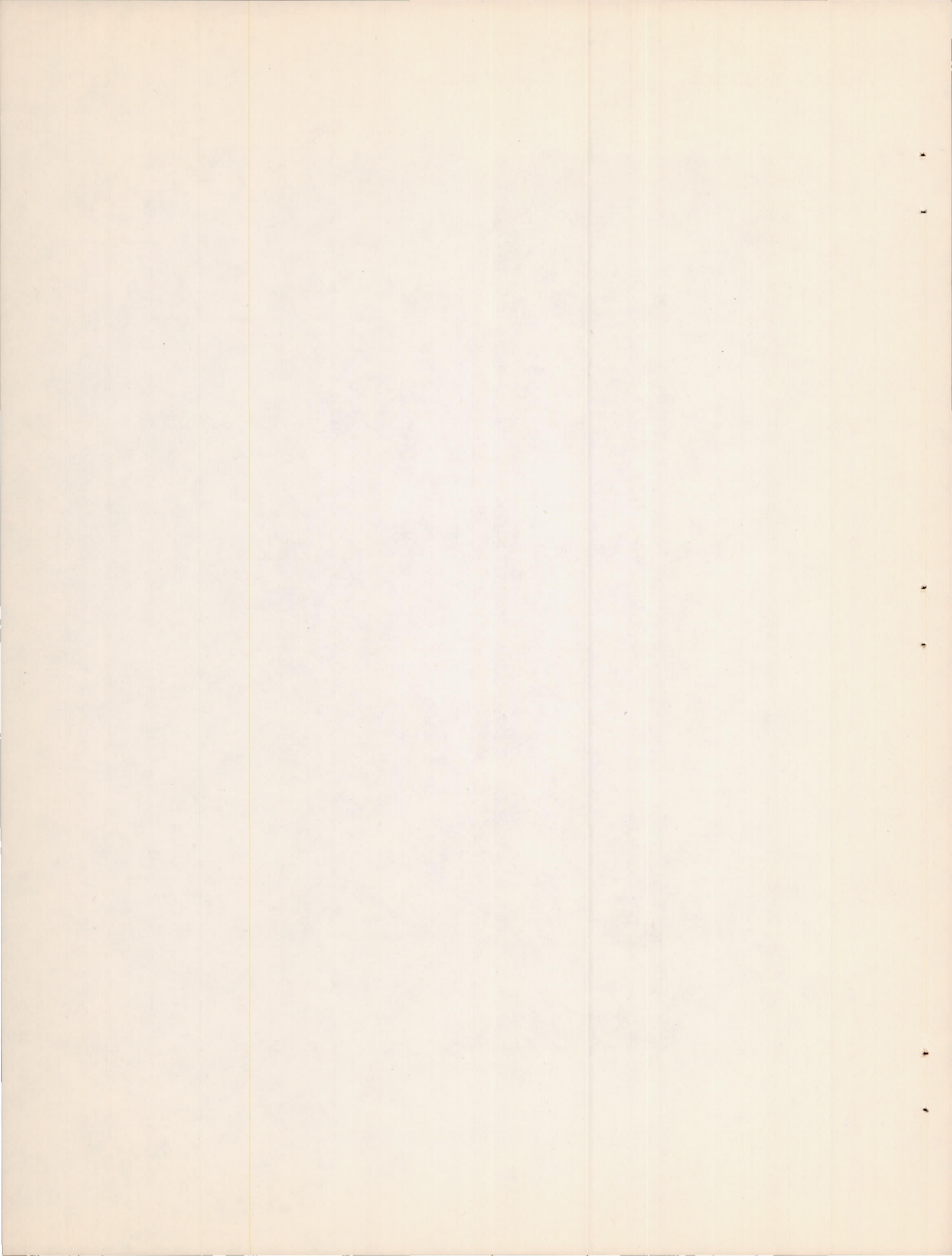
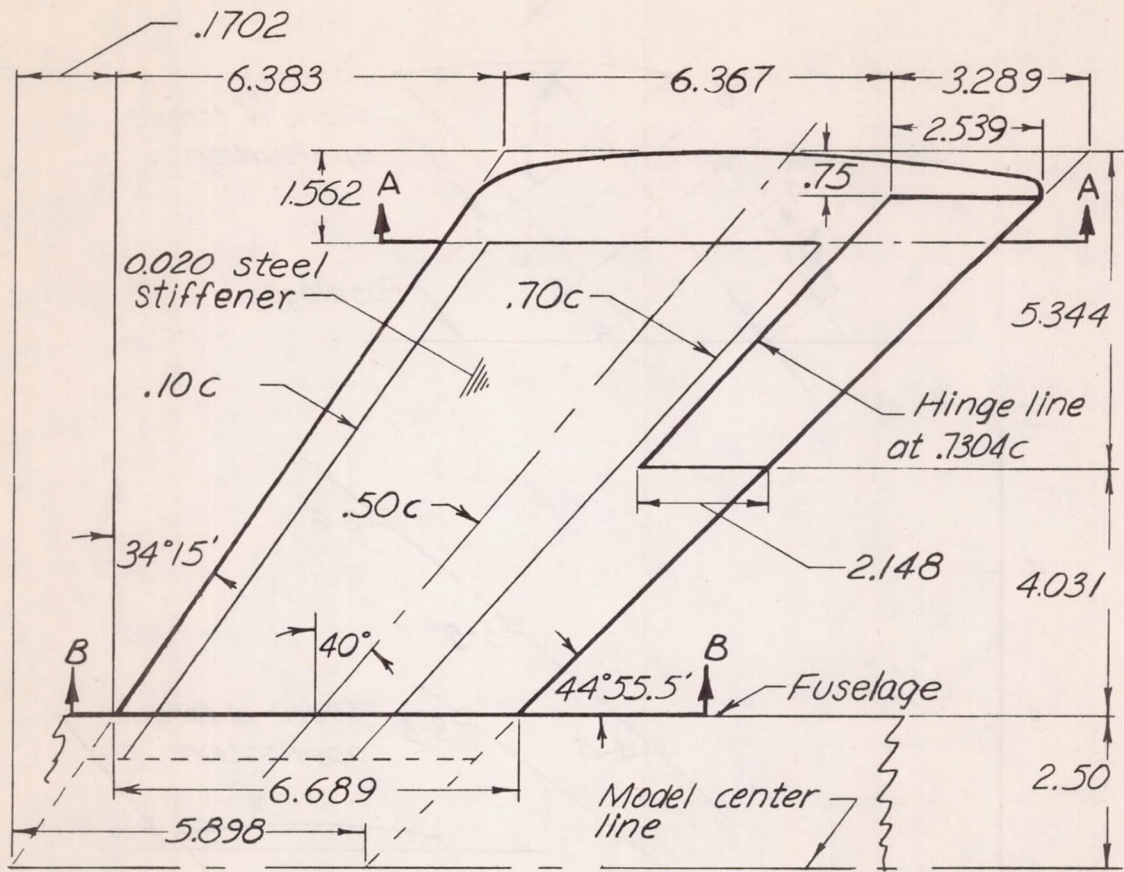


Figure 1.- Photograph of typical test vehicle.





Plan form

All dimensions are in inches

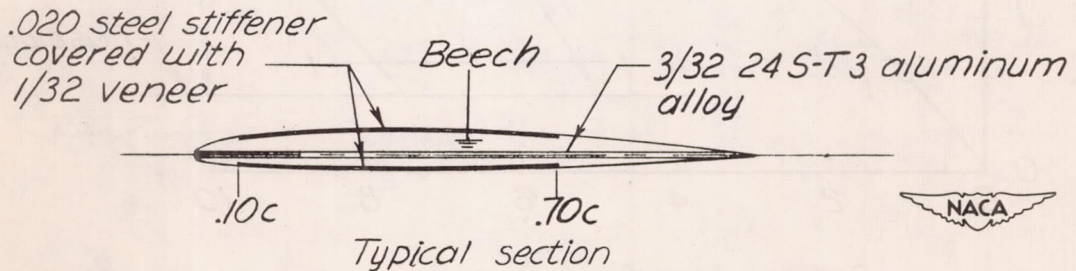


Figure 2.- Sketch of test wing. Airfoil section ordinates of A-A and B-B are given in table II.

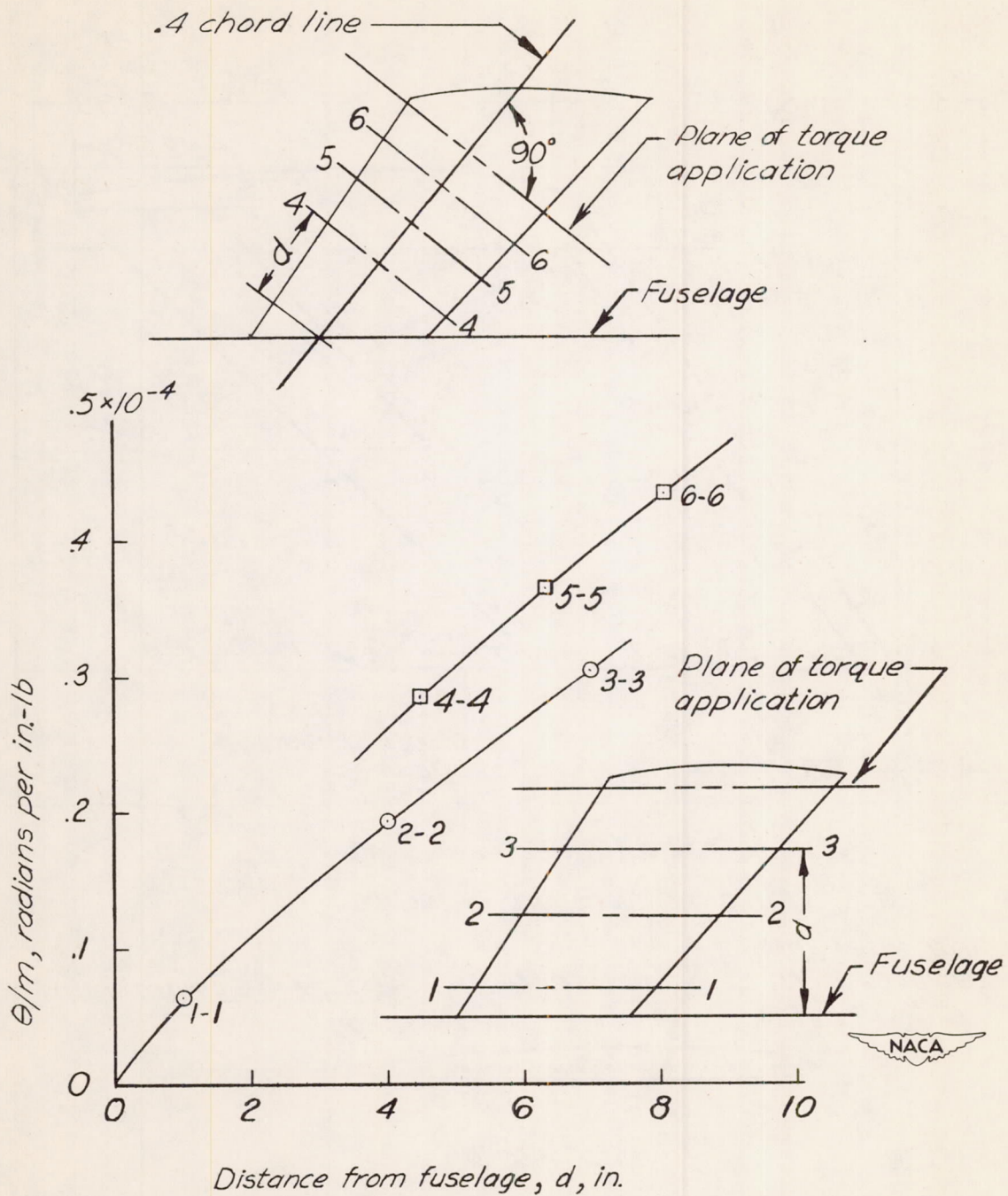


Figure 3.- Average measured variation of torsional rigidity with distance from fuselage.

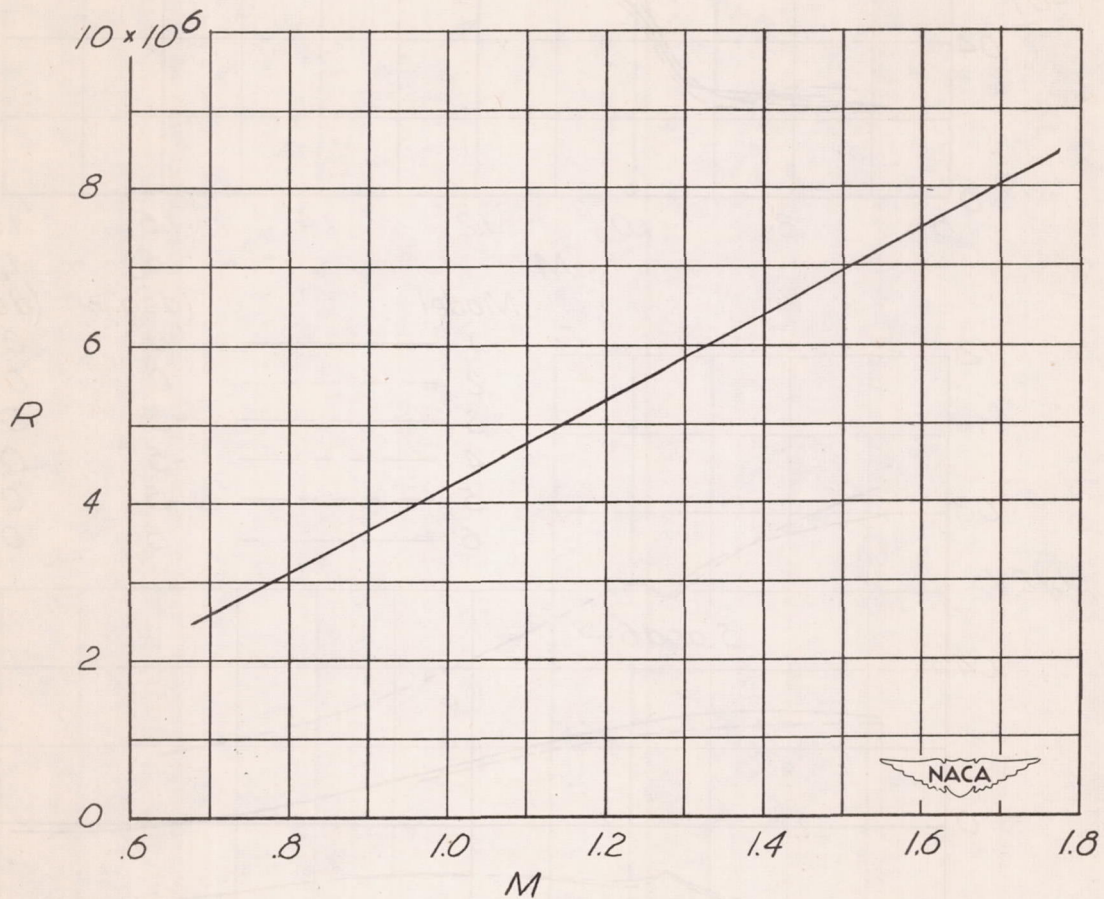


Figure 4.- Variation of Reynolds number with Mach number, based on an average exposed wing chord of 0.681 foot.

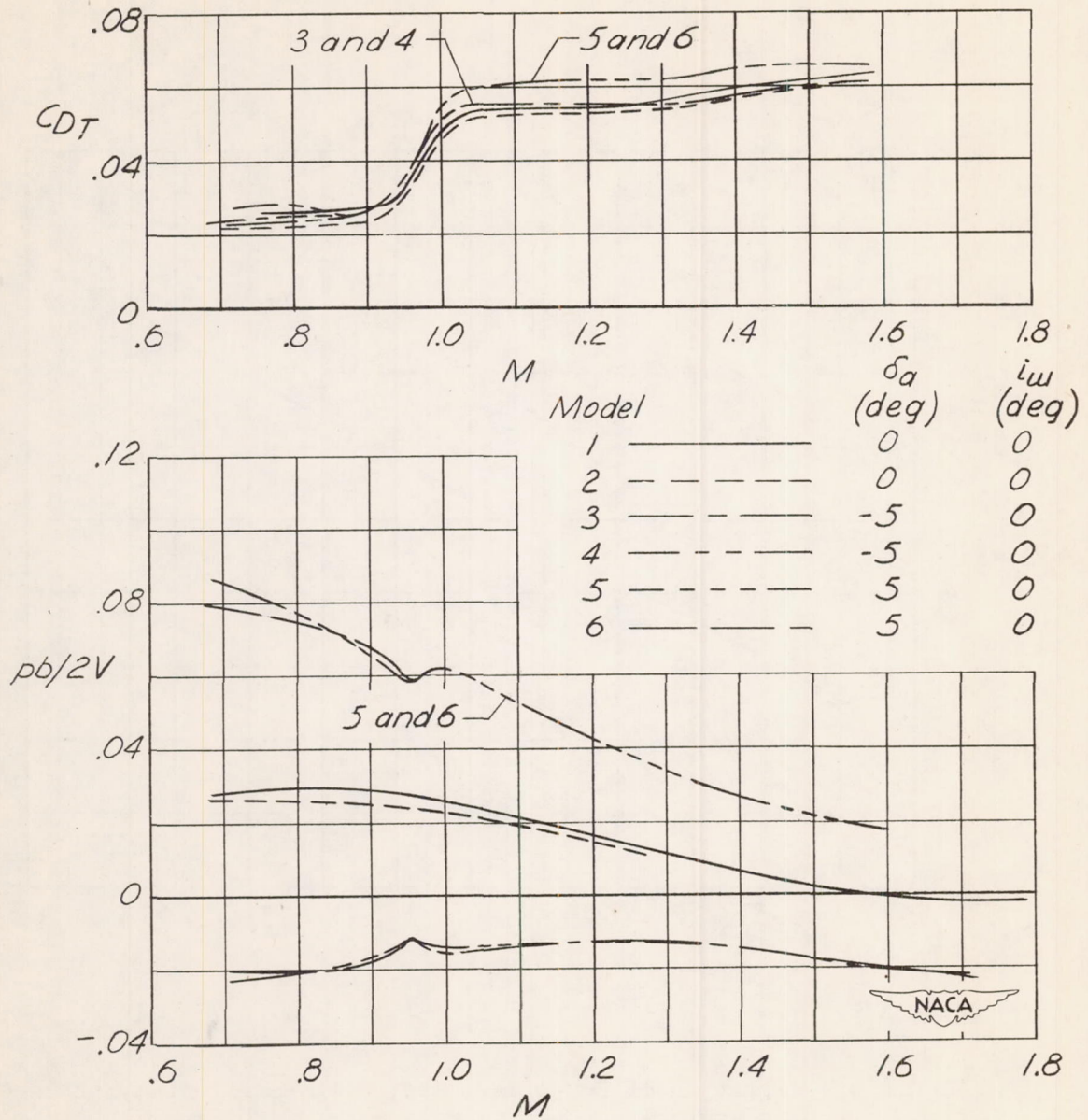


Figure 5.- Variation of rolling effectiveness parameter $pb/2V$ and total-drag coefficient C_{DT} with Mach number.

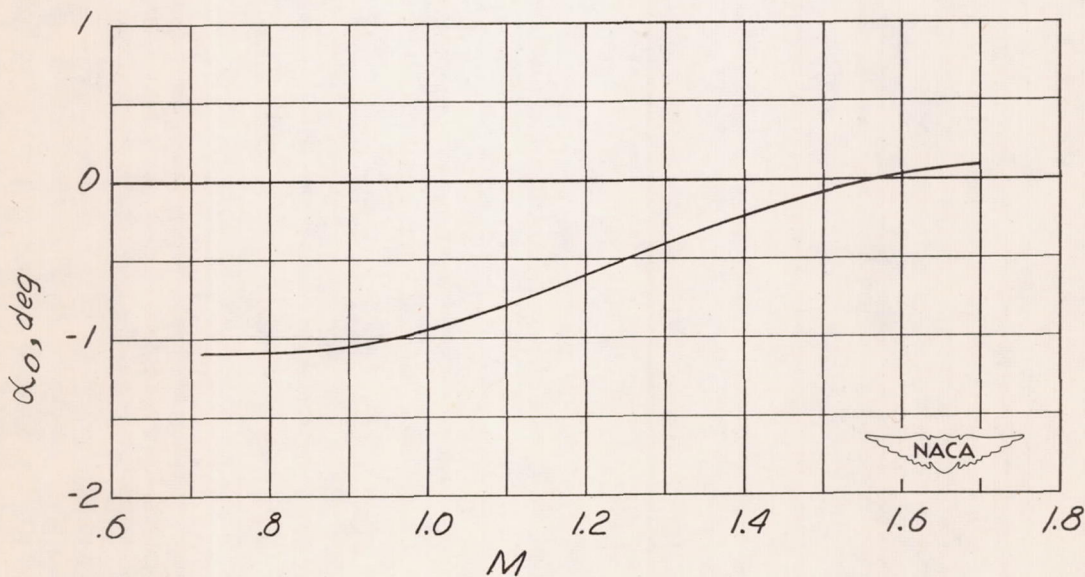
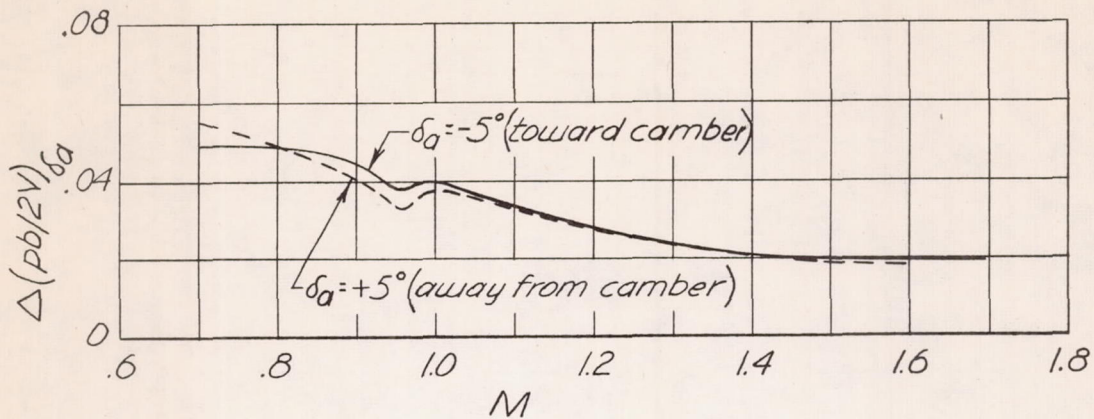


Figure 6.- Variation of aileron rolling effectiveness $\Delta(pb/2V)\delta_a$ and effective angle of attack for zero lift α_0 with Mach number.

